American Mineralogist, Volume 67, pages 1273–1289, 1982

Margaritasite: a new mineral of hydrothermal origin from the Peña Blanca Uranium District, Mexico

KAREN J. WENRICH, PETER J. MODRESKI, ROBERT A. ZIELINSKI AND JAMES L. SEELEY

U.S. Geological Survey
Box 25046, MS 916, Denver Federal Center
Denver, Colorado 80225

Abstract

Margaritasite, a Cs-rich analogue of carnotite, is a newly discovered uranium mineral that is part of the ore at the Margaritas deposit in the Peña Blanca uranium district near Chihuahua, Mexico. The margaritasite occurs as disseminated pore fillings and relict phenocryst linings within a rhyodacitic tuff breccia of the lower Escuadra Formation (Oligocene) and provides significant reserves of both uranium and cesium. It is a fine-grained yellow mineral and, with the possible exception of the index of refraction, is optically indistinguishable from carnotite. Margaritasite is most easily recognized by X-ray diffraction through a shift in the (001) reflection representing an increase, relative to carnotite, in the *c* dimension. This increase is due to the large Cs atom in sites normally occupied by K in the carnotite structure.

This Cs–K uranyl vanadate, with Cs:K about 5, is the natural equivalent of the compound $Cs_2(UO_2)_2V_2O_8$ synthesized by fusion (Barton, 1958). Chemical analyses of the mineral give the formula

$$(Cs_{1.38}(H_3O)_{0.35}K_{0.29})_{\Sigma 2.02}(UO_2)_{1.99}(V_2O_8)_{1.00}\cdot 1.07H_2O$$

corresponding to the generalized formula

$$(Cs,K,H_3O)_2(UO_2)_2V_2O_8\cdot nH_2O \text{ where } Cs > K,H_3O \text{ and } n \simeq 1$$

Unit cell parameters are $a = 10.514$, $b = 8.425$, and $c = 7.25$Å, $\beta = 106.01°$ ($P2_1/a$, $Z = 2$). Microprobe analyses of margaritasite and Cs-enriched carnotites synthesized by ion exchange of carnotite in aqueous CsCl solution at 200°C suggest a solid solution between carnotite and margaritasite, but X-ray powder patterns reveal that two discrete *c* dimensions exist with no intermediate value between them. The margaritasite has a (001) reflection at 12.7° (2θ) while that of carnotite lies at 13.8° (2θ); these peaks do not shift. It is likely that there are two distinct phases, perhaps as interlayered lamellae which are intergrown on a smaller scale than can be resolved by the electron microprobe beam.

The discovery of Cs-rich carnotite in the Peña Blanca uranium district provides important evidence for local hydrothermal or pneumatolitic activity during or after uranium mineralization. Data from the geochemical literature indicate that the high Cs:total alkali element ratios required to produce Cs-rich minerals can be generated and sustained only in high temperature environments. Synthesis experiments show that margaritasite can form by reaction of Cs-rich solutions with natural carnotite at 200°C, but the same reaction does not occur or is too slow to be observed in 61 days at 80°C. Nevertheless, it appears unlikely that margaritasite is part of the ore in any Colorado Plateau-type uranium deposit. Reported "carnotite" occurrences from uranium deposits of probable hydrothermal origin are likely sites for new discoveries of margaritasite.

Introduction

Margaritasite, a newly-recognized uranium mineral and a Cs-rich analogue of carnotite, is an ore mineral at the Margaritas deposit in the Peña Blanca uranium district near Chihuahua, Mexico. The recognition of margaritasite within these rocks is important for the characterization of this deposit and is of interest in the exploration for other deposits of similar origin. The physical and chemical con-

0003–004X/82/1112–1273$02.00

straints determined to be necessary for the formation of margaritasite can contribute to knowledge of the genesis of ore deposits hosting this mineral. The mineral and name margaritasite were approved by the Commission on New Minerals and mineral names of the International Mineralogical Association. Margaritasite is named after the Margaritas deposit where it was discovered. A specimen of margaritasite has been provided to the U.S. National Museum of Natural History, Washington, D.C.

Cesium-carnotite was first synthesized by a fusion technique, using metavanadate fluxes, by Barton (1958). This synthesis provided sufficiently large crystals that Appleman and Evans (1965) were able to determine the crystal structure of Cs-carnotite. The X-ray diffraction pattern of the synthetic Cs-carnotite was published by Barton (1958) and is very similar to that of margaritasite (which contains about 1 wt.% K_2O) except for a slightly larger *c*-dimension.

Geologic setting

The Peña Blanca district is located within the Basin and Range Province of Mexico approximately 70 km north of Chihuahua City in the north-central portion of Sierra Peña Blanca (Fig. 1). Sierra Peña Blanca lies among other fault-bounded ranges containing similar sequences of Tertiary volcanic units. A 300-m-thick Tertiary sequence of rhyolitic ash-flow tuffs and volcaniclastic sediments caps the bulk of this range. Three formations within this sequence contain ignimbrites constituting outflow facies from an as yet unidentified caldera source (Goodell, 1981). The uppermost (Mesa) and lowermost (Nopal) formations are particularly voluminous and of regional extent, being most widespread in the Sierra del Nido volcanic province to the west and northwest (Fig. 1). This range is the major volcanic source area in the region, and contains rocks which are compositionally and temporally more variable than rocks of the Peña Blanca range (Goodell, 1981). Although the older rhyolitic tuffs of Sierra Peña Blanca, Sierra Pastorias, and Majalca Canyon are not peralkaline (Table 1), the younger Campana and Cryptic Tuffs of the northern Sierra del Nido are (Dayvault 1980, Table 1; see also Table 1, this report). More information on the volcanic geology of the region can be found in Goodell and Waters, 1981.

At the Peña Blanca uranium district, the Tertiary volcanics overlie a regional continental molasse, the Pozos conglomerate, which rests unconformably on Cretaceous limestones. The volcanics have been dated by Alba and Chavez (1974) at 43.8±0.9 m.y. for the Nopal Formation, 38.3±0.8 m.y. for the Escuadra Formation, and 37.3±0.7 m.y. for the Mesa Formation (Fig. 1). The Peña Blanca volcaniclastic unit lies between the later two formations. Uranium mineralization occurs in stratiform and fracture-controlled deposits within the Escuadra and Nopal Formations.

Uranium deposits of Peña Blanca

The Peña Blanca uranium district is unusual for North America because of its geologic setting in silicic volcanic rocks. Over the past 20 years, numerous uranium occurrences at Peña Blanca have been systematically drilled and developed by underground mining (Goodell, 1981). In recent years, several of these have proven to be of commercial interest and are in active stages of development. Presently the Nopal 1 deposit is partially exploited, an incline is being driven into the Puerto III deposit and the Margaritas deposit is being prepared for exploitation by open-pit mining (Goodell, 1981). Based upon projected estimates of U resources, the Peña Blanca district could prove to be the most significant volcanic uranium district in North America. Reserves at the Margaritas deposit alone are believed to be 4.6 million pounds of U_3O_8 with an average ore grade of 0.103% (Gálvez and Vélez, 1974) along with molybdenum reserves at an average grade of 0.3% (Goodell *et al.*, 1978). In addition, the margaritasite provides a significant reserve of cesium.

The Margaritas deposit lies within a northwest-trending syncline (Goodell, 1981) in the lower Escuadra and underlying Nopal Formations (Fig. 2). This deposit lies at the intersection of two fracture zones along which most uranium occurrences of the Peña Blanca district occur: one trends northwest-southeast and the other north-south (Calas, 1977). A geologic cross section of this deposit with interpretations by the Instituto Nacional de Energia Nuclear shows the location of the analyzed sample of margaritasite (Fig. 2). Occurrences of margaritasite are by no means minor, being scattered on the surface toward the axis of the syncline. The other uranium ore minerals found in the Margaritas deposit are uranophane, betauranophane, autunite and weeksite (Goodell, 1981); all contain hexavalent uranium and are associated with anomalously high concentrations of Mo probably in powellite (Goodell, 1982) and V in metatyuyamunite (Goo-

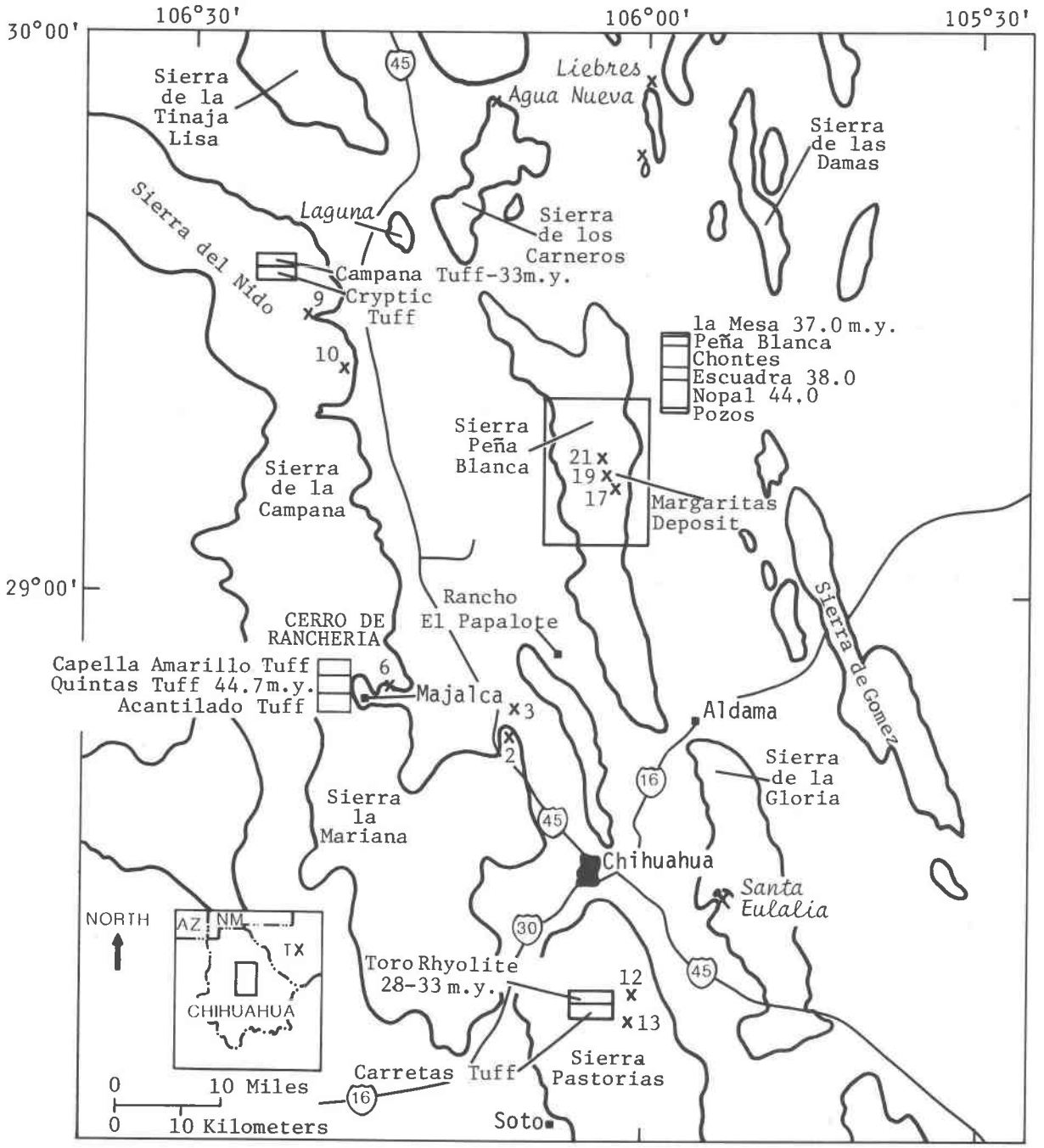

Fig. 1. Location map for the Peña Blanca Uranium District, Mexico, (located in the center of the diagram). Sample locations are shown for analyses listed in Table 1. The Margaritas deposit is located at site 19. The stratigraphic column for Sierra Peña Blanca is shown to the upper right of the area. The sample of margaritasite came from the Escuadra formation. (Modified from Goodell, 1981).

dell, 1982) as well as in margaritasite. No tetravalent U minerals have been observed in the Margaritas deposit, although uraninite occurs in the Nopal I deposit (Table 1). At the Margaritas deposit mineralization is structurally controlled, and is in two strata-bound environments, an altered vitrophyre and a breccia of reworked tuff clasts. Margaritasite occurs as pore fillings and phenocryst casts within the rhyodacitic breccia of reworked tuff clasts in the lower Escuadra Formation (Fig. 2). The boundary of margaritasite mineralization is gradational with hematitic, kaolinitic and silicic alteration scattered

Table 1. Chemical analysis of rocks from Sierra Peña Blanca and vicinity (oxides in percent, trace elements in ppm except where noted otherwise).

	19-G80	17-G80	21-G80	2-G80	3-B-G80	6-G80	9-A-G80	10-A-G80	12-A-G80	13-C-G80
SiO_2	68.1 %	41.7 %	63.7 %	72.3 %	69.4 %	72.5 %	72.5 %	73.2 %	69.2 %	68.6 %
Al_2O_3	12.0	6.01	11.7	14.2	13.8	12.6	11.0	10.4	15.1	13.8
Fe_2O_3	5.48	0.39	2.19	1.83	1.69	1.18	2.83	4.63	2.55	1.65
MgO	0.1	<0.1	<0.1	0.2	0.4	0.3	<0.1	<0.1	0.4	0.4
CaO	0.77	0.34	0.35	0.65	1.11	0.76	0.43	0.08	1.56	1.06
Na_2O	<0.2	<0.2	<0.2	3.4	4.6	3.8	4.1	0.9	4.1	4.7
K_2O	3.16	0.41	2.38	5.87	3.37	3.92	3.66	8.87	4.47	2.99
TiO_2	0.38	0.05	0.18	0.29	0.34	0.23	0.20	0.17	0.51	0.34
P_2O_5	0.3	<0.1	<0.1	<0.1	<0.1	<0.1	<0.1	<0.1	<0.1	<0.1
MnO	<0.02	<0.02	<0.02	0.08	0.07	0.06	0.09	0.12	0.06	0.08
LOI	4.62	6.94	5.7	0.99	4.64	3.56	3.95	0.56	1.51	4.75
U	7820 ppm	29 %	6.46%	23.8 ppm	5.47ppm	19.6 ppm	20.7 ppm	58.6 ppm	11.8 ppm	5.0 ppm
Th	30.3 *	H	H	15 *	13 *	36 *	39 *	111 *	12 *	13 *
F	0.06	0.09ppm	0.18ppm	0.07	0.05	0.03	0.13	0.10	0.06	0.05
S	0.33	0.18	0.01	0.03	<0.01	<0.01	<0.01	<0.01	0.04	0.01
As	1450	900	920	10	<0.5	<0.5	<0.5	20	5	<0.5
Se	-	15	<0.1	<0.1	<0.1	<0.1	<0.1	<0.1	<0.1	<0.1
Cs	2000	4	38	6	31	73	58	21	3	61
Li	24	33	22	32	15	26	90	154	38	17
Rb	150	6	188	198	163	324	350	542	143	185
Ag	0.92	<4.6	<4.6	<0.46	<0.46	<0.46	<0.46	<0.46	<0.46	<0.46
Au	<4.6	<22	<46	<4.6	<4.6	<4.6	<4.6	<4.6	<4.6	<4.6
B	15	5.1	14	12	5.8	34	38	17	12	7.1
Ba	754 *	202 *	96 *	1220 *	1030 *	123 *	55	26	1180 *	1720 *
Be	3.4	4.7	3.4	2.5	2.0	2.6	6.5	17	2.4	2.2
Bi	110	<46	H	<10	<10	<10	<10	<10	<10	<10
Cd	<20	<46	<10	<10	<10	<10	<10	<10	<10	<10
Ce	143 *	28 *	136 *	89 *	95 *	83 *	239 *	150 *	101 *	100 *
Co	2.6 *	<65	<65	<0.39*	0.66*	0.89*	<0.46	0.34*	2.6*	0.80*
Cr	28 *	17	4.1	0.50*	0.78	1.28*	0.98	0.66	1.51*	0.66*
Cu	27	70	29	<0.46	<0.46	1.1	<0.46	1.1	1.6	<0.46
Dy	2.3 *	1.5 *	17 *	6.4 *	7.2 *	6.4 *	19 *	51.8 *	8.7 *	7.3 *
Er	17	<4.6	<4.6	<4.6	<4.6	<4.6	<4.6	15	<4.6	<4.6
Eu	0.42*	0.12*	1.4 *	1.5 *	1.3 *	0.54*	0.2 *	0.6 *	2.0 *	1.5 *
Ga	23	H	H	12	10	9.6	17	30	14	11
Gd	<10	0.99*	7.9 *	7.1 *	7.2 *	7.2 *	19 *	36.9 *	10 *	7.4 *
Ge	1.9	<1.0	<1.0	1.1	1.0	1.4	1.7	5.8	1.8	1.4
Hf	14 *	300	<300	8.0 *	8.6 *	6.4 *	20 *	62.5 *	8.9 *	8.9 *
La	72 *	6.5 *	41 *	46 *	47 *	48 *	123 *	30 *	70 *	48 *
Lu	0.16*	0.16*	1.2 *	0.65*	0.69*	0.50*	1.84*	4.8*	0.68*	0.71*
Mo	>1500	520	<22	1.9	1.3	2.5	3.9	2.2	1.7	2.1
Nb	32	49	15	17	18	20	66	170	23	21
Nd	52 *	9 *	132 *	40 *	40 *	34 *	108 *	46 *	59. *	42 *
Ni	40	<100	23	1.7	4.7	1.5	4.8	1.5	2.8	1.7
Os	<22	<93	<93	<22	<22	<22	<22	<22	<22	<22
Pb	91	1600	460	21	19	22	33	160	30	22
Pd	<1.0	<10	<10	<1.0	<1.0	<1.0	<1.0	<1.0	<1.0	<1.0
Pr	<68	<200	<200	<68	<68	<68	<68	<68	<68	<68
Pt	<10	<30	<30	<10	<10	<10	<10	<10	<10	<10

Table 1. (continued)

	19-G80	17-G80	21-G80	2-G80	3-B-G80	6-G80	9-A-G80	10-A-G80	12-A-G80	13-C-G80
Sb	4.93*	<46	<46	1.1 *	0.4 *	0.8 *	0.9 *	8.6 *	0.4 *	0.4 *
Sc	6.09*	<6.5	<6.5	5.9 *	3.9 *	3.2 *	1.0 *	1.0 *	4.7 *	3.8 *
Sm	6.4 *	2.2 *	26 *	8.0 *	7.8 *	6.9 *	21. *	22. *	11 *	8.1 *
Sn	19	<4.6	<4.6	<4.6	<4.6	<4.6	<4.6	23	<4.6	<4.6
Sr	3060 *	57	240	72	225 *	64	22	24	156 *	146 *
Ta	1.9 *	<500	<500	1.7 *	1.6 *	2.5 *	5.0 *	16.0 *	1.5 *	1.6 *
Tb	0.58*	0.22*	2.3 *	1.1 *	1.2 *	<46	3.1 *	7.3 *	1.5 *	1.2 *
Tl	<1000	<4.6	<4.6	<4.6	<4.6	13	<4.6	<4.6	<4.6	<4.6
Tm	<9.3	<46	1.7 *	<4.6	0.7 *	<4.6	1.9 *	5.7 *	0.8 *	0.8 *
V	1100	H	68	3.5	3.6	8.0	<1.0	<1.0	24	6.0
Y	16	<40	47	35	35	26	90	240	44	37
Yb	0.98*	0.95*	10.3 *	4.0 *	4.6 *	3.5 *	12. *	33 *	4.5 *	4.6 *
Zn	72	<140	<140	40	59	59	110	250	51	48
Zr	380	980	470	240	328 *	150	753 *	1930 *	375 *	351

Other elements which were also determined but were less than the detection limit are:
Ho <10 ppm In <50 ppm Ir <46 ppm Re <46 ppm Rh <2.2 ppm Ru <10 ppm W <46 ppm
H = Analytical interference
- = Not determined
Methods of analysis:
1. Major element oxides, loss on ignition (LOI), and Se: X-ray fluorescence
2. U, Th: Delayed neutron activation
3. Cs, Rb, As: Atomic Absorption
4. Li: Induction Coupled Plasma - Optical Emission Spectrometry
5. S: Sulfur Analyzer
6. F: Specific Ion Electrode
7. "*": Neutron activation analysis
8. All other elements: Semi-quantitative emission spectroscopy
Sample Descriptions (sample locations shown on figure 1):
19-G80: Margaritas Deposit, Peña Blanca district, Escuadra Formation; sample of ore hosting the margaritasite.
17-G80: Nopal I Deposit, Peña Blanca district, Nopal Formation; sample of ore, predominantly uraninite and soddyite.
21-G80: Puerto V Deposit, Pena Blanca district, Nopal Formation; sample of ore containing weeksite after feldspar.
2-G80: Cerro Jesus Maria; welded tuff, vent breccia at Bellavista.
3-B-G80: Cerro Jesus Maria; Sacramento Bluff Rhyolite (believed to be equivalent to the lower part of the Nopal Formation).
6-G80: Majalca Canyon; basal vitrophyre of the Quintas Tuff.
9-A-G80: Sierra del Nido; basal vitrophyre of the Cryptic Tuff.
10-A-G80: Sierra del Nido: Campana Tuff riebeckite rhyolite.
12-A-G80: Sierra Pastorias; Toro Rhyolite.
13-C-G80: Sierra Pastorias; Basal vitrophyre of the Toro Rhyolite.

irregularly throughout the deposit (P. C. Goodell, oral comm., 1981). The ore forming processes at Margaritas are presently not well understood. Bazan Barron (1978) considers the deposits of Sierra Peña Blanca to be of Laramide age and hydrothermal origin.

Trace element chemistry of volcanic rocks from and around Sierra Peña Blanca

The trace element chemistry (Table 1, column 1) of the tuff breccia, which hosts the margaritasite, shows several elements in addition to Cs, V, and U to be in anomalously high concentrations (Table 1). Molybdenum, As, Sr, and Ag are exceptionally high, and in fact Mo is considered a byproduct of uranium mining at the Margaritas deposit. Other elements which are anomalously high as compared to average crustal abundances for rhyolites are: B, Bi, Ce, Cr, Er, Ni, Pb, S and Sc.

High contents of uranium in ash flow tuffs are not unique to Sierra Peña Blanca, but also occur at Sierra del Nido where the Campana Tuff contains up to 59 ppm uranium (Table 1); this unit is also high in rare earth elements such as Dy and Er. Although the low Na_2O content suggests that this tuff has been altered, the high Th content and a Th/U ratio of 2.6 suggest that the enrichment of uranium is mostly primary. Both the Campana Tuff and Cryptic Tuff contain higher concentrations of F and Li than do the volcanics from adjacent ranges. High concentrations of Cs, in excess of 50 ppm, occur in the basal vitrophyres of the Cryptic Tuff (Sierra del Nido), the Toro Rhyolite (Sierra Pastorias) and the Quintas Tuff (Majalca Canyon). The Quintas Tuff is

believed to be correlative with the Nopal Formation to the east in Sierra Peña Blanca (Goodell, 1981). Vitrophyres of the Nopal and Escuadra Formation likewise have high Cs concentrations (P. C. Goodell, written comm., 1981) particularly as compared to the tuff units. Although some of these vitrophyres have high U, there does not appear to be a significant correlation between Cs and U.

Petrography of the tuff breccia

Margaritasite occurs as fine-grained yellow aggregates up to 1 mm in size within interstices of the rhyodacitic tuff breccia. Some of the hematite-stained breccia clasts are porphyritic tuff containing pumice fragments, and others are dominantly composed of partly devitrified glass shards; the interstitial material is neither hematite stained nor does it contain glass shards, but is comprised primarily of quartz and kaolinite with minor sanidine. Minor amounts of quartz, much lesser amounts of sanidine, and sparse, highly altered biotite phenocrysts occur in the porphyritic breccia clasts. The breccia clasts are fractured in places and are filled by interstitial kaolinite. What appears to have been plagioclase has been altered to clay. Accessory minerals include apatite, zircon, and pyrite. The clasts are entirely volcanic, generally lapilli size, indurated, and well sorted; the rock appears to be reworked. The matrix does not appear to be volcanic suggesting that the brecciation was sedimentary in origin, although any transport could not have been too great judging from the good preservation of the tuff clasts.

The margaritasite occurs in the interstices either as (1) linings within relict phenocrysts (probably biotite), occasionally with kaolinite forming the outer euhedral border with an equally thick layer of margaritasite encasing a hollow core (Fig. 3a), or (2) as amoeboid aggregates (Fig. 3b). The individual crystals of margaritasite are 1 to 3 μm in size and are in some places intergrown with quartz (Fig. 4). Because of its fine-grained nature, the margaritasite

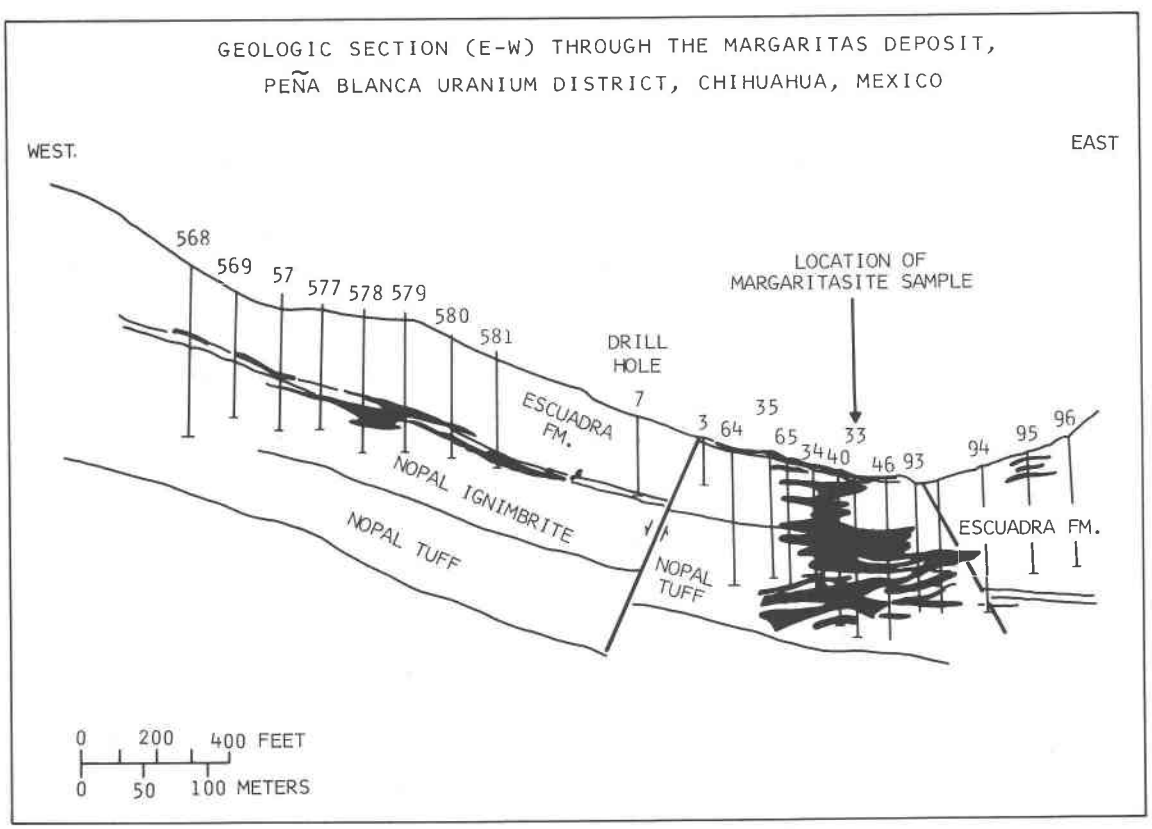

Fig. 2. Section constructed from drill hole information. Location and identifying number of drill holes are shown. Distribution of uranium ore is indicated in black, as interpreted by the Instituto National de Energia Nuclear from gamma-ray logging of drill holes (unpublished data). The margaritasite sample was collected in the vicinity of drill hole #33 (arrow). Margaritasite is present at the surface from approximately drill hole #46 to #64. (Diagram from Goodell, 1981, with additions).

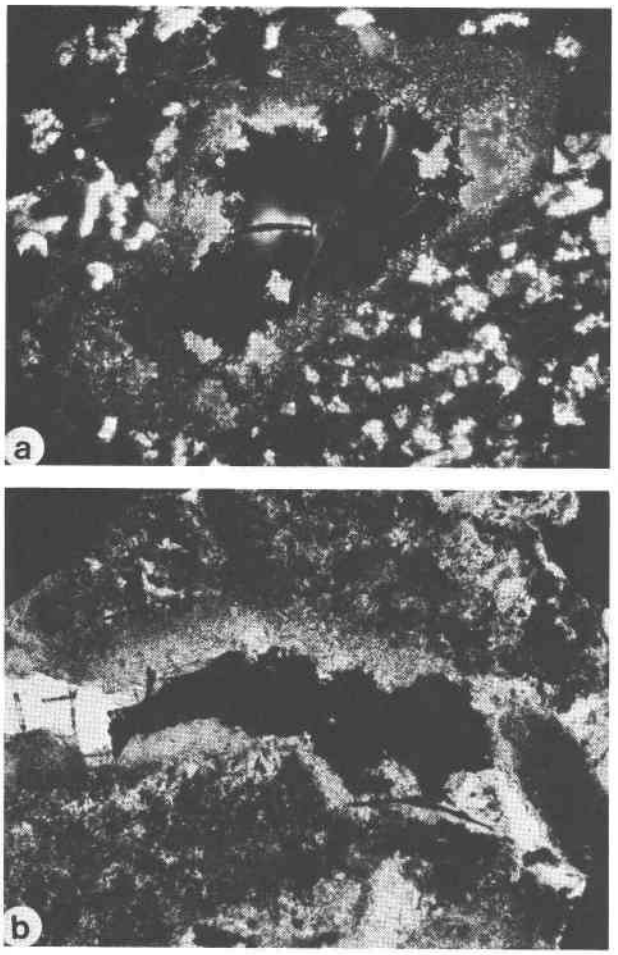

Fig. 3 (a) Photomicrograph of a relict phenocryst in the tuff breccia with an outer lining of kaolinite and an inner lining of margaritasite (lighter toned material). Relict phenocryst outer length equals 1.38 mm (width of photo equals 1.46 mm); crossed nicols. (b) Photomicrograph of an amoeboid margaritasite aggregate surrounded by an alteration halo. Length of aggregate equals 0.87 mm (width of photo equals 1.37 mm); uncrossed nicols.

appears grey and nonpleochroic in transmitted light, although, in an exceptionally thin section, yellow-brown absorption colors are present under crossed nicols; reflected light is required to yield the characteristic yellow carnotite color. Margaritasite is optically indistinguishable from carnotite. The small crystal size, the biaxial nature of the mineral, and its very high indices of refraction have prevented measurement of the refractive indices. The synthetic anhydrous Cs analogue of carnotite has $\alpha < 1.83$, $\beta = 2.49$, $\gamma = 2.70$, $2V = 45°30'$ (Barton, 1958). The margaritasite is not noticeably fluorescent in ultraviolet light. The difficulty in purifying sufficient quantities of margaritasite combined with the small grain size and very high density have prevented measurement of the density; the calculated density of margaritasite is 5.41 g/cm^3 while the calculated density of synthetic $Cs_2(UO_2)_2V_2O_8$ is 5.52 g/cm^3.

X-ray crystallography

The synthetic Cs analogue of carnotite is isostructural with synthetic carnotite (Barton, 1958; Appleman and Evans, 1965). Both are monoclinic, space group $P2_1/a$ with unit cell content $2[M_2(UO_2)_2V_2O_8]$. Margaritasite has a powder diffraction pattern very similar to the synthetic Cs carnotite reported by Barton (1958). The intensities and d-spacings of the powder diffraction maxima of margaritasite and those of the calculated pattern for Cs carnotite (Powder Diffraction File, card 25-1218) are remarkably similar, while distinct from those of natural (potassium) carnotite (Table 2).

The d-spacings and intensities observed for margaritasite were obtained with Cu$K\alpha$ (nickel filter) radiation, $\lambda = 1.54178$Å. The d-spacings were averaged from multiple diffractometer recordings calibrated with quartz as an internal standard. The sample of margaritasite on which the powder pattern was obtained also contained trace amounts of quartz, which makes the true intensity of the Cs-carnotite peaks observed at 3.344Å and 1.820Å uncertain; the true intensities may be lower than those reported here.

Unit-cell parameters (Table 3) and calculated d-spacings (Table 2) were obtained from a least-squares refinement (using a program written by

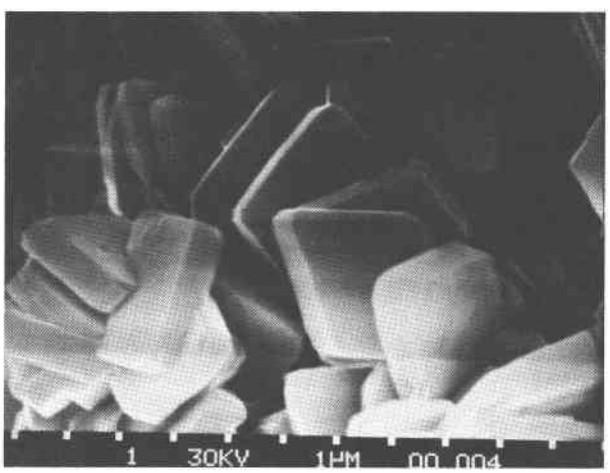

Fig. 4. Scanning Electron Microscope photograph of margaritasite crystals. The distance between tick marks is 1 μm.

Table 2. X-ray powder diffraction data for margaritasite (Margaritas deposit, Peña Blanca district, Chihuahua, Mexico). (diffractometer: Cu$K\alpha$ radiation, λ = 1.54178Å, Ni filter; quartz internal standard. Last column shows selected d-spacings for natural carnotite (Frondel, 1958) for comparison.)

hkl	d(calc.)	d(obs.)	I(obs.)	2θ observed CuKα	Natural carnotite	Synthetic+ Cs-carnotite
001*	6.971	6.965	100	12.71	6.56	7.033
110*	6.471	6.454	10	13.72		6.481
$\bar{1}11$*	5.225	5.215	4	17.00		5.254
200*	5.053	5.048	12	17.57	5.12	5.049
111*	4.373	4.362	14	20.36	4.25	4.393
020*	4.213	4.208	7	21.11		4.225
$\bar{2}11$*	4.146	4.142	14	21.45		4.158
021*	3.605	3.600	70	24.73	3.53	3.622
002*	3.485	3.489	60	25.53		3.517
211 $\bar{2}02$	3.343 3.330	3.344[x]	70[x]	26.66	3.25	3.351
220*	3.236	3.231	50	27.61		3.240
$\bar{3}11$ $\bar{2}21$	3.174 3.155	3.164	50	28.20		3.177 3.165
310*	3.128	3.129	35	28.53	3.12	3.127
221 $\bar{1}22$	2.754 2.744	2.752	6	32.54		2.762
130 $\bar{3}12$	2.706 2.696	2.702	17	33.16		2.709
311*	2.615	2.616	10	34.28	2.594	2.618
400*	2.527	2.527	3	35.52		2.525
$\bar{2}31$*	2.419	2.421	4	37.14		2.426
003	2.324	2.336	4	38.54		2.344
$\bar{4}21$*	2.224	2.224	5	40.56		2.225
$\bar{3}31$*	2.172	2.172	3	41.57		2.176
330*	2.157	2.157	14	41.88		2.160
040*	2.106	2.105	6	42.96		2.112
$\bar{2}23$*	2.068	2.069	6	43.75		2.068
$\bar{5}11$*	2.040	2.040	9	44.40		
$\bar{4}03$,$\bar{1}41$	2.008	2.007	4	45.18		
510,331	1.965	1.967	6	46.15		
$\bar{5}12$ 141 240	1.950 1.948 1.944	1.947	12	46.66		
$\bar{2}41$*	1.926	1.928	4	47.14		
241 520 402 $\bar{4}32$	1.823 1.822 1.821 1.817	1.820[x]	7[x]	50.11		
$\bar{6}02$*	1.713	1.712	3	53.53		
$\bar{5}31$*	1.683	1.684	5	54.48		

a = 10.514 std. error = .003
b = 8.425 std. error = .003
c = 7.252 std. error = .005
β = 106.01°
V = 617.48 Å^3 std. error = 0.44 Å^3

Values of d(calc) obtained from refinement based on cell parameters given above, using 23 reflections; space group = $P2_1/a$, with non-extinction conditions ($h0l$) h=2n, ($0k0$) k=2n. * = reflections used in cell refinement.

[x]The intensities reported here for the 3.344 Å and 1.820 Å peaks may be slightly high because of contribution from the (101) (3.34 Å) and (112) (1.817 Å) peaks of a trace of admixed quartz. However, a powder photograph obtained with a Gandalfi camera on a quartz-free sample of margaritasite still showed these same peaks with comparable intensity.

+Weak lines not observed in the margaritasite pattern are omitted from the calculated Cs-carnotite data from Powder Diffraction File card 25-1218. Higher angle lines of Cs-carnotite are omitted because the effect of the small difference in unit cell dimensions becomes increasing magnified with higher angles, and it is thus difficult to correlate lines between margaritasite and synthetic Cs-carnotite.

Table 3. Comparison of properties—K and Cs carnotites

	K carnotite synthetic, anhydrous (Barton, 1958)	K carnotite natural, Utah (Donnay and Donnay, 1955)	Cs carnotite synthetic, anhydrous (Barton, 1958)	Margaritasite (present work)
Space group	$P2_1/a$	$P2_1/a$	$P2_1/a$	$P2_1/a$
Z	2	2	2	2
a (in Å)	10.47	10.47	10.51	10.514 (3)
b (in Å)	8.41	8.41	8.45	8.425 (3)
c (in Å)	6.59	6.91	7.32	7.252 (5)
β	103.8°	103.7°	106.1°	106.01°
V (in Å^3)	563.5	590.8	624.3	617.5 (4)
n(α)	1.77	--	<1.83	--
n(β)	2.01	--	2.49	--
n(γ)	2.09	--	2.70	--
2V	53.5°	--	45.5°	--
d(calc.)	4.99	4.91	5.52	5.40
d(obs.)	4.95	4.70	5.48	--

VanTrump and Hauff, 1978, and based on the algorithm of Appleman and Evans, 1973) of the powder data using 23 reflections, with the non-extinction conditions $h = 2n$ for $(h0l)$ and $k = 2n$ for $(0k0)$, appropriate for the space group $P2_1/a$. Agreement between observed and calculated d-spacings is very good, with computed standard errors of 0.003 for a, 0.003 for b, and 0.005 for c, and 0.44Å^3 for the unit-cell volume; assignment of observed reflections in the cell refinement was aided by comparison with a calculated powder pattern for margaritasite supplied by Howard Evans (written comm., 1981) in addition to the calculated pattern from the Powder Diffraction File (card 25-1218).

The unit-cell parameters (Table 3) agree well with those of synthetic Cs-carnotite (Powder Diffraction File card 25-1218 or Barton, 1958). The presence of Cs is most strongly manifested in the c dimension, which expands in response to the substitution of Cs ions for the smaller K ions (ionic radii for 12-coordinated Cs+ is 1.96Å and that for 12-coordinated K^+ is 1.68Å, estimated by Whittaker and Muntus, 1970, p. 952) that reside between layers of $[(UO_2)_2V_2O_8]_n^{-2n}$ (Appleman and Evans, 1965).

Carnotite can have a variable water content of between zero and three molecules of H_2O per $[M_2(UO_2)_2V_2O_8]$ formula unit, and hydration or dehydration of carnotite is reported to affect the c cell dimension (Donnay and Donnay, 1955). They reported that the c length of a natural carnotite increased from 6.59Å to 6.63Å when subjected to an atmosphere of 100% humidity for one day. Margaritasite that was placed in a 100% humidity atmosphere at 25°C for 88 hours showed an analytically insignificant increase in c from 7.25Å to 7.26Å. Heating the margaritasite in air (30% to 55% relative humidity at 27°C) for a total of 68 hours at successively increasing temperatures between 100°C and 500°C decreased the c dimension of margaritasite to 7.17Å. The initial X-ray powder patterns were obtained on material that was stored in air at about 25°C and 30% relative humidity. Natural carnotite from the Colorado Plateau showed no significant change in the c dimension of 6.63Å upon exposure to 100% humidity and 25°C, and a decrease in c to 6.52A upon heating to 500°C. Donnay and Donnay (1955) report that carnotite can undergo partial dehydration upon grinding; after 4 minutes of grinding in an agate mortar, no change was observed in c of margaritasite, and a small, non-significant increase (6.63 to 6.64Å) was observed in c of carnotite.

Chemical analysis

Chemical analysis of margaritasite was done by both standard laboratory methods and by election microprobe. The microprobe analyses were made on an ARL-SEMQ automated electron probe, at 15 kV accelerating potential and 10 nA sample current. The microprobe data were corrected using a version of the MAGIC IV program (Colby, 1968). A counting time of 40 seconds on each peak and 4 seconds on background was used. Standards used were KCl for K, pollucite for Cs, Rb, Si, and Al, albite for Na, calcite for Ca, uranium metal for U, vanadium metal for V, orpiment for As, barite for Ba, and celestite for Sr. The $K\beta$ X-ray fluorescence lines of potassium and vanadium were used instead of $K\alpha$ to avoid interference by overlapping lines of U and Cs. Multiple analyses (14) were made on individual as well as different aggregates of margaritasite. The results showed the aggregates to be relatively homogeneous (Table 4). The margaritasite totals for the four major components only sum to 92 wt.%; water probably accounts for no more than another 3 wt.% and the remainder of the determined trace elements sum to an insignificant total. This discrepancy in the total may be a matrix effect due to a lack of appropriate standards for the various elements, but is more likely a result of the imperfect surface polish attainable on the fine-grained soft margaritasite aggregates. The mean Cs_2O/K_2O ratio by weight of margaritasite aggregates and individual grains equals 11.3±4, so that the Cs_2O is always significantly greater than the K_2O content. In the natural margaritasite from the Peña Blanca district, there is minimal heterogeneity in the Cs_2O/K_2O

concentration and no evidence for a complete solid solution to the carnotite end member.

Standard laboratory analyses were made on purified samples of margaritasite which were separated from the bulk rock by methylene iodide heavy mineral separations, Franz isodynamic separations, and hand picking. Determinations of U and V were done by inductively coupled argon plasma atomic emission spectrometry (ICAP-AES) using a Jarrell-Ash Model/1160 direct-reading polychromator; K and Cs were determined by atomic absorption spectrophotometry using a Perkin-Elmer Model 603 spectrometer with an air-acetylene flame. Matching-matrix synthetic standards were prepared from standard solutions of high-purity materials, with each sample and standard solution containing 2000 ppm Li to further buffer potential matrix differences. Replicate analyses were made on three separate splits of the margaritasite, each weighing approximately 10 mg, with resultant coefficients of variation of 0.81% for K, 0.65% for Cs, 0.30% for U, and 1.58% for V. Sample dissolution was accomplished by HF, HNO_3, $HClO_4$ digestion. Water determinations were made on a Perkin-Elmer 240B

Table 4. Chemical analyses of margaritasite (in wt.%)

	Electron Microprobe			Standard laboratory methods (Atomic Absorption spectrometry unless otherwise indicated)		
	Ave.	Recalculated to 100% (assume 2.5% water)	Range of 14 determinations	Ave.	Recalculated to 100%	Range of 3 determinations
Cs_2O	17.6 %	18.7	15.6 - 19.0	17.0 %	19.7	16.9 - 17.1
K_2O	1.63	1.73	1.07 - 2.14	1.20	1.39	1.19 - 1.20
UO_3	55.4	58.9	51.7 - 58.4	49.6	57.5	49.5 - 49.8 *
V_2O_5	17.0	18.1	16.1 - 18.9	15.9	18.4	15.6 - 16.0 *
H_2O	--	(2.5)	-- --	2.5	2.9	-- --***
Total	91.63	99.9		86.2	99.9	
Na	<.06%		<.06%	<.001%		-- --
Rb	<.12		<.12	.08		-- --
Ca	.33		.27 - .37	.3		-- --
Sr	.07		<.0008 - .24	.03		-- --
Ba	.19		<.0009 - .32	.16		-- --
Si	.14		.05 - .25	--		-- --
Al	.02		<.0005 - .06	<.001		-- --
As	<.06		<.06	--		-- --
Mo	--		--	<.08		-- --
Mn	--		--	.011		-- --
Fe	--		--	.0004		-- --
Zn	--		--	.04		-- --
Mg	--		--	.02		-- --
Li	--		--	<.001		-- --
P	--		--	<.01		-- --
Ti	--		--	.5 **		-- --
Cr	--		--	.015**		-- --
Y	--		--	.01 **		-- --
Zr	--		--	.015**		-- --
Ga	--		--	.002**		-- --

* Determinations made by ICAP-AES
** Semiquantitative emission spectroscopy
*** Carbon-hydrogen-nitrogen analyzer
-- Not determined

carbon-hydrogen-nitrogen analyzer. Determinations of trace elements were done both by atomic absorption spectrophotometry and by semiquantitative emission spectroscopy; the method used for each element is indicated on Table 4. Unfortunately the fine-grain size (approximately 1–3 μm) of the margaritasite made it impossible to totally separate from the quartz with which it appears to be intimately intergrown. Thus, the sum of Cs_2O + K_2O + UO_3 + V_2O_5 + H_2O only equals 86.2%; the remainder is probably quartz, as the entire sample went into solution when treated with hydrofluoric acid. Nevertheless, as can be seen from Table 4, the average element determinations for margaritasite separated from 5 pounds of host rock are in proportion to those determined by the electron microprobe on individual grains. In fact, when both analyses are recalculated to 100% (assuming 2.5% H_2O for the microprobe analysis) the results are in excellent agreement (Table 4).

The ideal formula for margaritasite is $(Cs,K)_2(UO_2)_2V_2O_8{\cdot}nH_2O$ where Cs > K and n varies from 0 to 3. The empirical formula based on 2 vanadium atoms and the standard laboratory analysis shown in Table 4 is

$$(Cs_{1.38}K_{0.29})_{\Sigma 1.67}(UO_2)_{1.99}(V_2O_8)_{1.00}{\cdot}1.62H_2O.$$

Unfortunately, this results in an alkali charge deficiency. Both the microprobe and atomic absorption analyses showed a consistent range in total alkalies rather than the expected 2.00. This appears to be a real deficiency and cannot be accounted for by other alkalies such as Rb, Na, Li or by alkaline earths such as Mg, Ca, Sr, or Ba; all of these elements summed to less than 0.1 formula unit although Ca approaches 0.1 (Table 4). The total formula unit contributed by Ca (0.086), Ba (0.013), Rb (0.011), Mg (0.009), Zn (0.007), Sr (0.004), and Mn (0.002) is 0.132. These remaining cation vacancies are believed to be filled by H_3O^+ ions; because of the uncertainty in which sites the trace elements (Table 4) belong or if they occur in admixed impurities, all vacant alkali sites have been assigned to H_3O^+ (oxonium). This reduces the total H_2O, which could be as high as 1.5 assuming all 0.132 trace element formula units went into this site. The empirical formula based on the wet chemical data is therefore

$$(Cs_{1.38}(H_3O)_{0.35}K_{0.29})_{\Sigma 2.02}(UO_2)_{1.99}(V_2O_8)_{1.00}{\cdot}1.07H_2),$$

and the ideal formula is

$$(Cs,H_3O,K)_2(UO_2)_2V_2O_8{\cdot}nH_2O$$

where Cs > H_3O,K and n ≃ 1.

The empirical formula based on the microprobe data, ignoring water, is:

$$(Cs_{1.31}K_{0.36})_{\Sigma 1.67}(UO_2)_{2.03}(V_2O_8)_{0.98}$$

The apparent presence of oxonium ions in margaritasite may be compared to other oxonium-containing layer structures such as boltwoodite, $K(H_3O)UO_2(SiO_4){\cdot}nH_2O$ (Stohl and Smith, 1973), torbernite group minerals (Ross and Evans, 1965) hydrous uranyl oxides (Sobry, 1971), illite, and hydromicas. An oxonium end-member in the carnotite–metatyuyamunite group vanuranylite, $(H_3O,Ba,Ca,K,Pb)_{1.6}(UO_2)_2(VO_4)_2{\cdot}4H_2O$ (?) has been reported by Buryanova *et al.* (1965), and an apparent oxonium end-member analogous to carnotite was synthesized by Barton (1958). Published analyses have shown minor amounts of Ca in carnotite (Donnay and Donnay, 1955; Frondel, 1958).

Cs-carnotite synthesis and results

An attempt was made to synthesize cesium-rich carnotite by reaction of natural carnotite from the Colorado Plateau with 0.1 M CsCl solution (pH of 5.6) at 80°C and 200°C (Table 5). The natural carnotite contained less than 0.01 Cs atoms per formula unit but was contaminated by quartz, with minor amounts of calcite, potassium feldspar and albite. Reactants were encapsulated in pinch-sealed or welded Pt capsules which were loaded into reaction vessels made of screw-cap polyethylene bottles (80°C) or lengths of stainless steel tubing with compression fittings at each end. Approximately 10 ml of CsCl solution was also loaded in the reaction vessels to provide additional reagent in the

Table 5. Experimental conditions and products

Experiment	Seal	Wt. carnotite (mg)	Wt. 0.1M CsCl (mg)	T°C	Duration (days)
1	pinch	10	>400	80	14
2	pinch	10	>400	80	61
4	welded	10	200	200	14
5	welded	10	200	200	61
6	welded	10	200	200	209

event of capsule leakage and to act as a pressure transmitting agent. Loaded, sealed capsules which were used in the 200°C experiments were weighed before and after the experiment; no leaks were detected. Constant temperature environments (±5°C) were provided by an air-circulating drying oven (80°C) and a muffle furnace (200°C). Experiment pressure was ambient vapor pressure at the experimental temperatures. In all experiments the ratio of Cs/K in the system (solid + liquid) exceeded 3.0. At the end of an experiment the reaction vessel was cooled with water to room temperature in approximately 5 minutes. The recovered solid phases were washed with H_2O, dried at room temperature and submitted for X-ray diffraction (XRD) and election microprobe analysis.

Microprobe analyses and atomic proportions of the natural carnotite starting material and the 5 ion exchange products are shown in Table 6. In addition to the elements listed, Na, Rb, and As were also determined but are not shown because their concentrations were below the limit of confident determination (0.01–0.2 wt.% oxide). The apparent deficiency of alkalies in all of these analyses may indicate the presence of oxonium ions in the alkali site.

Figure 5 shows the changes in Cs/(K + Cs) between the 5 experimental runs, the natural carnotite, and margaritasite. The two experimental runs at 80°C (14 and 61 day durations) produced carnotites with small, less than 0.05 mole fraction Cs, but measurably increased Cs contents. The carnotite starting material had a significantly smaller but measurable Cs content (0.02 mole fraction Cs). The 200°C products showed increasingly higher contents of Cs with increasing duration of the experiment (Fig. 5). After 209 days at 200°C some of the experimental products had a Cs/(K + Cs) ratio of greater than 0.7 mole fraction Cs which is equivalent to the lowest Cs mole fraction of the Peña Blanca margaritasite (Fig. 5).

Microprobe traverses across several carnotite grains in the 200°C, 209 day experiment at 0.5 μm steps, using an electron beam of approximately 1 μm in diameter, showed an irregular zonation of Cs_2O/K_2O, with the number of K atoms per formula unit ranging from about 0.2 to 1.2 (equivalent to about 1 to 5.5 wt.% K_2O). There was no evidence of Cs-rich margins on K-rich cores.

The potassium and sodium feldspars present as an impurity with the natural carnotite starting material do not appear to have incorporated a significant

Table 6. Microprobe analyses of synthesized Cs–carnotites. Calculated atomic proportions (on the basis of U + V = 4) shown in parentheses

	Number of analyses in average	Cs_2O	K_2O	UO_3	V_2O_5	CaO	SrO	BaO	SiO_2	Al_2O_3	Total*
Natural Carnotite	9	0.12 (0.007)	8.27 (1.454)	69.29 (2.006)	21.89 (1.994)	0.33	0.14	0.05	0.02	0.12	100.23
Experiment #1 80°C 14 days	4	0.75 (0.045)	8.36 (1.517)	67.25 (2.009)	21.18 (1.991)	0.18	0.01	0.03	0.03	0.06	97.85
Experiment #2 80°C 61 days	5	0.85 (0.052)	8.51 (1.557)	67.10 (2.022)	20.88 (1.978)	0.21	0.06	0.05	0.04	0.05	97.73
Experiment #4 200°C 14 days	6	2.45 (0.154)	8.68 (1.628)	65.90 (2.035)	20.22 (1.965)	0.16	0.01	0.04	0.03	0.12	97.62
Experiment #5 200°C 61 days	4	4.13 (0.256)	7.90 (1.468)	65.18 (1.993)	20.86 (2.007)	0.34	0.00	0.03	0.04	0.04	98.52
Experiment #6 200°C 209 days	9	12.83 (0.873)	4.80 (0.979)	59.75 (2.004)	18.91 (1.996)	0.16	0.04	0.07	0.17	0.05	96.77

*Water content not determined

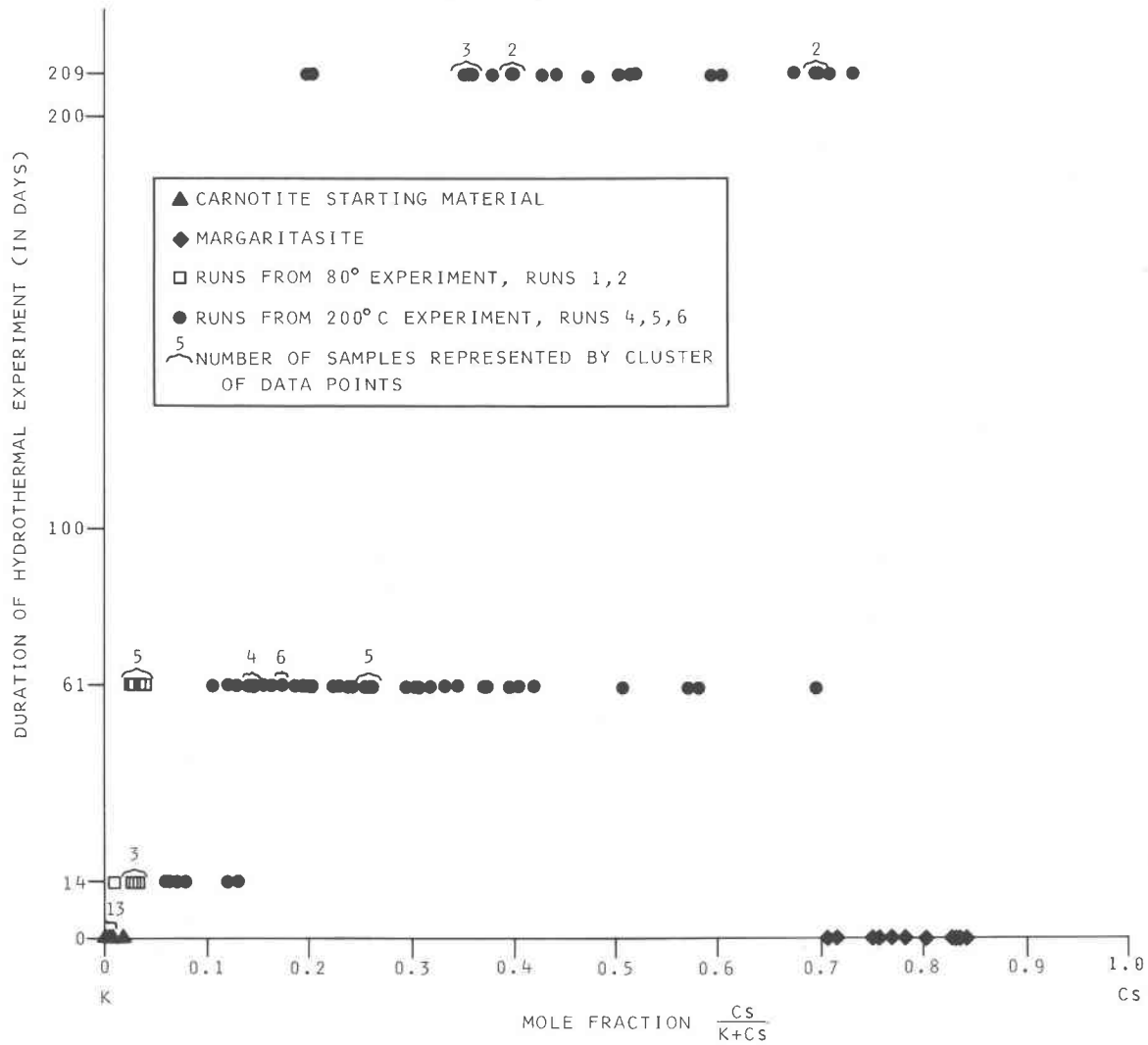

Fig. 5. Variation of the mole fraction of Cs/(K + Cs) with duration of the Cs–carnotite synthesis experiments.

amount of Cs during the experimental run; microprobe analysis of spots near the edge of feldspar grains in run 6 (200°C and 209 days) showed less than 0.03 wt.% Cs_2O. The Ca and Si present in the runs (from the calcite, quartz, and/or feldspar impurities in the starting material) did react with some of the carnotite in experiment 6 to produce a Ca uranyl vanadate phase as well as a Ca uranyl silicate phase; the vanadate was probably tyuyamunite or meta-tyuyamunite, but due to its paucity its identity could not be confirmed on the X-ray diffraction pattern. In addition, globules and glassy-appearing coatings (on carnotite, quartz, and feldspar) of a Cs–Al-silicate of pollucite composition ($CsAlSi_2O_6$) were observed on the microprobe in all three of the 200°C runs; this material has the appearance of a product which precipitated during the quenching of the run. Alternatively the pollucite may have grown during the run as a stable reaction product of the CsCl solution + quartz + feldspar. The presence of several strong pollucite diffraction lines in the powder pattern from experiment 6 (pollucite is most abundant in this run) confirm the identification based on chemistry. Pollucite has been found to be a common phase precipitated from heated Cs-bearing aqueous solutions in contact with aluminosilicates (McCarthy *et al.*, 1978). Despite the observed formation of new phases from the apparent breakdown of some carnotite, a significant proportion of the carnotite obviously underwent ion exchange as can be observed in Table 6 by the reasonable formula proportions.

The X-ray powder diffraction data for the natural carnotite and the experimental products were obtained from repeated scans between 10° and 50° 2θ with Cu$K\alpha$ radiation scanned at 1/2° (2θ)/min. The X-ray patterns are shown in Figure 6 where they are compared with the pattern for margaritasite. The sample of natural carnotite and consequently its experimental products have a strongly enhanced (001) peak caused by preferred orientation of the carnotite platelets on the mounting medium.

Unit cell parameters for the experimental products were calculated from the powder X-ray diffraction data (Table 7). The X-ray data for the products run at 80°C yield cell dimensions which are not analytically distinguishable from those of the starting carnotite. Powder patterns (Fig. 6) of the 14 and 61 day, 80°C experiments show a very small peak at about 12.36° (2θ); this peak does *not* appear to be the (001) reflection of a margaritasite phase. The same weak peak was observed at 12.40° (2θ) in powder patterns of the natural, Cs-free carnotite, and it appears to be due to some trace inpurity phase. In contrast, the X-ray diffraction data on the 200°C products show two distinct (001) peaks, one for carnotite at 13.8° (2θ) and one for margaritasite at 12.7° (2θ).

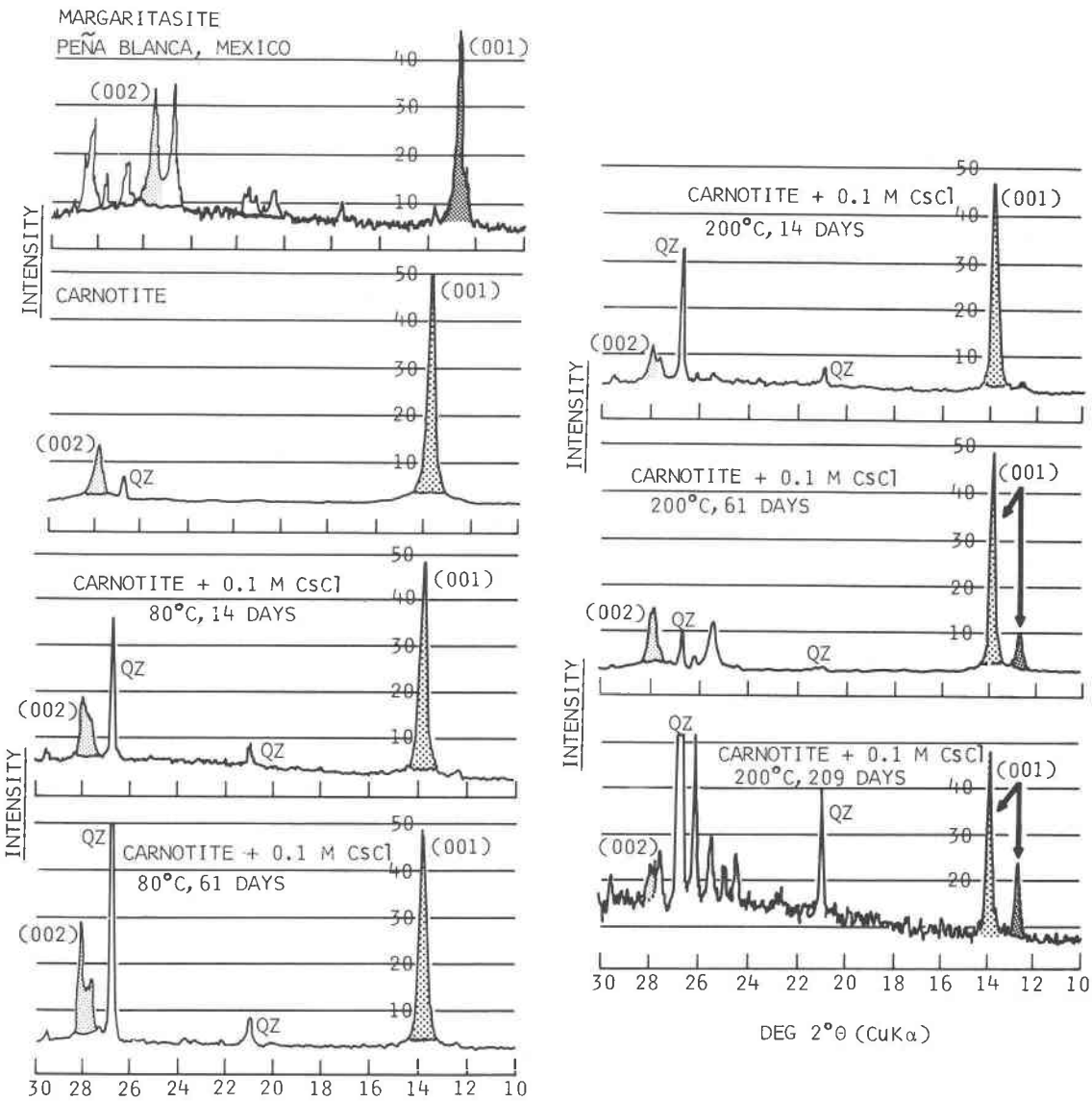

Fig. 6. X-ray powder diffraction patterns for margaritasite, Colorado Plateau carnotite and synthesized Cs–carnotite.

Table 7. Unit cell dimensions of natural and synthetic margaritasite and carnotite (-- = not determined)

	a(Å)	b	c	β(°)
Margaritasite phase				
natural marg.	10.514	8.425	7.250	106.01
Experiment 6	10.61	8.42	7.31	106.1
Experiment 5	10.54	8.41	7.30	105.6
Experiment 4	--	--	7.30*	--
Carnotite phase				
Experiment 6	--	--	6.62*	--
Experiment 5	10.43	8.42	6.59	103.5
Experiment 4	10.41	8.43	6.62	103.8
Experiment 2	10.52	8.41	6.65	104.7
Experiment 1	10.52	8.42	6.65	104.8
natural carn.	10.45	8.41	6.63	104.1

*c calculated from the (001) and (002) reflections only

For the series of 200°C experiments the diffraction lines for the Cs-rich phase (of which the (001) and (002) reflections are the most pronounced) are barely discernable in the 14-day run and increasingly strong in the 60- and 209-day runs. The products of all three experiments at 200°C (4, 5, 6) are mixtures of a high-Cs and a low-Cs carnotite, each with distinct d-spacings which do not shift with varying Cs content. These data suggest that there is an abrupt structural transition from carnotite to margaritasite which may be triggered by the incorporation of a threshold amount of Cs.

Discussion

According to the chemical data shown in Figure 5 the synthetic Cs-rich carnotites are not as homogenous as margaritasite although no discrete zoning is present. Even the 200°C, 209-day experiment includes two measured products with anomalously low Cs_2O/K_2O ratios. Only low Cs-carnotite grains were detected by the microprobe in the material from experiment 4 (200°C, 14 days) (Fig. 5), but the presence of weak (001) reflections at 6.97Å (Fig. 6) indicates the presence of a small, incipient quantity of Cs-enriched carnotite in this experiment also.

The electron microprobe analyses suggest that an asymmetric, limited solid solution may exist between $K_2(UO_2)_2V_2O_8{\cdot}nH_2O$ and $Cs_2(UO_2)_2V_2O_8{\cdot}nH_2O$ (see Fig. 5). At 200°C this solid solution appears to be between $Carn_{100}Marg_0$ and $Carn_{27}Marg_{73}$ and at 80°C only between $Carn_{100}Marg_0$ and $Carn_{96}Marg_4$. The composition of margaritasite suggests that the solid solution exists up to $Carn_{14}Marg_{86}$ at some unknown temperature of formation. However, only two (001) reflections are observed; that is a discrete increase in the *c* lattice dimension occurs from 6.6Å to 7.3Å with no intermediate values. This may be due either to (1) a sudden *c*-axis increase when a critical number of the large Cs atoms are stuffed between the layers of $[(UO_2)_2V_2O_8]_n$ (this structural change occurs somewhere between $Carn_{80}Marg_{20}$ and $Carn_{41}Marg_{59}$) or (2) an extremely fine intergrowth of discrete phases of margaritasite and carnotite which is below the resolution of the electron microprobe beam. Nevertheless, a K mole fraction of at least 0.2 is acceptable into the margaritasite structure; analyses of the natural margaritasite yield K contents up to this concentration with no evidence of the carnotite (001) reflection in the margaritasite powder diffraction pattern.

Genetic implications for the Peña Blanca deposit

The discovery of Cs-rich carnotite in the Peña Blanca uranium district provides important evidence for local hydrothermal or pneumatolitic activity during or after uranium mineralization. Data from the geochemical literature (summarized below) indicate that the high ratios of Cs:total alkali elements which are required to produce Cs-rich minerals can be generated and sustained only in high temperature environments.

The mobility of Cs in low temperature ground water is severely restricted by adsorptive and ion exchange uptake by clays and zeolites (Ames, 1960; Jenne and Wahlberg, 1968; Chelischev, 1976). Reported concentrations of Cs in ground and surface water are generally less than 0.001 ppm (Wedepohl, 1970). These observations explain why Cs enrichment has never been reported in carnotites from low temperature Colorado Plateau uranium deposits. In contrast, thermal waters in young rhyolitic rocks of New Zealand contain <0.1 to 2.6 ppm dissolved Cs (Ellis and Mahon, 1964). Experiments designed to model the generation of such Cs concentrations showed that leaching of rhyolite glass by aqueous solutions at 400–600°C produces nearly quantitative removal of Cs in two weeks time (Ellis and Mahon, 1964). Additional experimental measurements of Cs partitioning between feldspar and an aqueous phase at 400–800°C showed that Cs strongly favors the aqueous phase (Eugster, 1955). Synthesis experiments in this study indicate that in 0.1 M CsCl solutions margaritasite can form from carnotite precursors within 6 months at 200°C.

Crystalline rhyolites (felsites) are typically de-

pleted in Cs relative to juxtaposed comagmatic vitrophyres, (Lebedeva and Shatkova, 1975; Zielinski, *et al.* 1977). Consistently large cesium depletions in felsites show no positive correlation with sample age, and thus suggest that Cs is liberated during or shortly after high temperature devitrification. High Cs concentrations (over 50 ppm) occur in vitrophyres but not in the associated felsites, of volcanic rocks from Sierra Peña Blanca and the adjacent regions of Sierra del Nido and Sierra Pastorias (Table 1). The availability of Cs in a high temperature gaseous or liquid phase is evidenced by the formation of Cs minerals such as pollucite $(Cs,Na)(AlSi_2O_6)\cdot H_2O$ in pegmatites. Gaseous transport of Cs as a complex with fluoride is suggested by the formation of $(K,Cs)BF_4$ and $CsBF_4$ in volcanic sublimates (Wedepohl, 1970; Shatkov, 1971).

High Cs abundance in the vicinity of uranium deposits is not unique to the Peña Blanca uranium district. Uranium and Cs are similarly incompatible elements in magmatic crystallization processes and tend to be enriched in the more silicic magmas. Walker (1981) has demonstrated a significant correlation between U and Cs in Tertiary rhyolites of the northern basin and range. This correlation also occurs within other ore deposits located in late stage magmatic rocks. Rytuba and Conrad (1981) have reported that Cs values are in excess of 100 ppm within rhyolites from the McDermitt, Nevada, uranium district, and that rhyolites hosting uranium deposits show an excellent positive correlation with Cs. Although the background Cs levels are lower (less than 20 ppm) in the Marysvale, Utah, area the Cs content is elevated in rocks which occur near uranium deposits, such as the uranium ore at the Prospector IV mine (Wenrich, unpublished data, 1980). This U and Cs correlation within late stage magmatic products suggests that ore deposits rich in U and Cs may well have a magmatic source.

Based on the above discussion it is unlikely that margaritasite will be found in low-temperature uranium deposits such as those of the Colorado Plateau. Conversely "carnotite" occurrences in uranium deposits of hydrothermal origin are probable margaritasite localities.

Acknowledgments

The authors wish to thank Joseph F. Mascarenas who assisted with the X-ray diffraction work, mineral separations, and data tabulation, and spent many hours hand picking impurities from the margaritasite sample. Ralph P. Christian provided valuable instruction during the electron microprobe analyses. James G. Crock performed the atomic absorption determinations for trace elements in the margaritasite and F. W. Brown determined the water content. Eugene E. Foord provided valuable advice on the crystallographic work as well as some of the standards for the electron microprobe analysis. We thank Deane K. Smith, Howard Evans, Edward Dwornik, and Philip C. Goodell for useful discussions. Analysts who contributed to the data in Table 1 were H. T. Millard, Jr., R. B. Vaughn, S. W. Lasater, B. A. Keaten, Z. Hamlin, D. Kobilis, J. S. Wahlberg, J. W. Baker, J. E. Taggart, J. G. Crock, C. A. Gent, H. G. Neiman, and R. Anderson. Thanks also goes to Paul B. Barton, Jr., Howard T. Evans, Jr., Daniel E. Appleman, and Malcolm Ross for time spent reviewing the manuscript and providing useful additions. The Colorado Plateau carnotite used in the Cs–carnotite synthesis experiments was supplied by Harry C. Granger. A special thanks to Howard Evans for sharing with us his calculated X-ray powder pattern for margaritasite.

References

Alba, L. A. and Chavez, Rafael (1974) K–Ar ages of volcanic rocks from the central Sierra Peña Blanca, Chihuahua, Mexico. Isochron/West, 10, 21–23.

Ames, L. L. (1960) The cation sieve properties of clinoptilolite. American Mineralogist 45, 689–700.

Appleman, D. E. and Evans, H. T., Jr. (1965) The crystal structures of synthetic anhydrous carnotite, $K_2(UO_2)_2V_2O_8$, and its cesium analogue, $Cs_2(UO_2)_2V_2O_8$. American Mineralogist 50, 825–842.

Appleman, D. E. and Evans, H. T. (1973) Indexing and Least-Squares Refinement of Powder Diffraction Data. National Technical Information Service, Washington, D. C., 9214.

Barton, P. B., Jr. (1958) Synthesis and properties of carnotite and its alkali analogues. American Mineralogist 43, 799–817.

Bazan Barron, Sergio (1978) Genesis y depositacion de los Yacimientos de molibdeno y uranio, en el Distrito de Villa Aldama, Chihuahua. Boletin Sociedad Geologica Mexicana, 39, 25–33.

Buryanova, E. Z., Strokova, G. S., and Shitov, V. A. (1965) Vanuranylite, a new mineral: Zapiski Vsesoyuznogo Mineralogicheskogo Obshchestva, 94, 437–443.

Calas, Georges (1977) Les phenomenes d'alteration hydrothermale et leur relation avec les mineralisations uraniferes en milieu volcanique: le cas des ignimbrites tertiaires de la Sierra de Peña Blanca, Chihuahua (Mexique). Scientific Geologists Bulletin, 30, 3–18.

Chelischev, N. F. (1976) Ion exchange properties of natural high silica zeolites, (abs). Zeolite 76, An International Conference on the Occurrence, Properties and Utilization of Natural Zeolites, Tucson, Arizona, 22–23.

Colby, J. W. (1968) Quantitative microprobe analysis of thin insulating films. Advances in X-Ray Analysis, 11, 287–305.

Dayvault, R. D. (1980) Peralkaline ash-flow tuffs in Santa Clara Canyon, north of Chihuahua City, Mexico, a possible source rock for uranium. American Association of Petroleum Geologists Abstract, Southwest section, 24.

Donnay, Gabrielle and Donnay, J. D. H. (1955) Contributions to the crystallography of uranium minerals. United States Geological Survey Trace Element Investigations Report 507, 1–42.

Ellis, A. J. and Mahon, W. A. J. (1964) Natural hydrothermal systems and experimental hot-water/rock interactions. Geochimica et Cosmochimica Acta, 28, 1323–1357.

Eugster, H. P. (1955) Distribution of trace elements. Carnegie Institute of Washington Year Book Geophysics Laboratory Reports, 54, 112–114.

Frondel, Clifford (1958) Systematic mineralogy of uranium and thorium. United States Geological Survey Bulletin 1064.

Gálvez, L. and Vélez, C. (1974) Uranium and its projected use in nuclear generation of electricity in Mexico—Summary. American Association of Petroleum Geologists Memoir, 25, 522–524.

Goodell, P. C. (1981) Geology of the Peña Blanca uranium deposits, Chihuahua, Mexico. In P. C. Goodell and A. C. Waters, Eds., Uranium in Volcanic and Volcanoclastic Rocks, p. 275–291. American Association of Petroleum Geologists Studies in Geology #13.

Goodell, P. C., Trentham, R. C., and Carraway, Kenneth (1978) Geologic setting of the Peña Blanca uranium deposits, Chihuahua, Mexico. In C. D. Henry and A. W. Walton, Eds., Formation of Uranium Ores by Diagenesis of Volcanic Sediments, IX-1–IX-38. Department of Energy Open-File Report GJBX-22(78).

Goodell, P. C. and Waters, A. C. (1981) Uranium in Volcanic and Volcanoclastic Rocks. American Association of Petroleum Geologists Studies in Geology #13.

Jenne, E. A. and Wahlberg, J. G. (1968) Role of certain stream-sediment components in radioion sorption. United States Geological Survey Professional Paper 433-F.

Lebedeva, L. I. and Shatkova, L. N. (1975) The distribution of Li, Rb and Cs in acid volcanic rocks. Geochemistry International, 12, 226–232.

McCarthy, G. J., White, W. B., Roy, Rustum, Scheetz, B. E., Komarneni, S., Smith, D. K., and Roy, D. M. (1978) Interactions between nuclear waste and surrounding rock. Nature, 273, 216–217.

Ross, Malcolm and Evans, H. T., Jr. (1965) Studies of the torbernite minerals (III): Role of the interlayer oxonium, potassium, and ammonium ions, and water molecules. American Mineralogist, 50, 1–12.

Rytuba, J. J. and Conrad, W. K. (1981) Petrochemical characteristics of volcanic rocks associated with uranium deposits in the McDermitt caldera complex. In P. C. Goodell and A. C. Waters, Eds., Uranium in Volcanic and Volcanoclastic Rocks, p. 63–72. American Association of Petroleum Geologists Studies in Geology #13.

Shatkov, G. A. (1971) The mode of occurrence of cesium in felsic volcanic glasses. Geochemistry International, 8, 553–556.

Sobry, R. (1971) Water and interlayer oxonium in hydrated uranates. American Mineralogist, 56, 1065–1076.

Stohl, F. V. and Smith, D. K. (1973) The crystal structures of boltwoodite and weeksite. (abstr.) Geological Society of America, Abstracts with Programs, 5, 824.

VanTrump, G., Jr., and Hauff, P. L. (1978) Least-squares refinement of powder diffraction data for unit cell parameters. United States Geological Survey Open-File Report 78-431.

Walker, G. W. (1981) Uranium, thorium, and other metal associations in silicic volcanic complexes of the northern basin and range, a preliminary report. United States Geological Survey Open-File Report 81-1290.

Wedepohl, K. H. (1970) Handbook of Geochemistry. II/4, Springer-Verlag, New York.

Whittaker, E. J. W., and Muntus, R. (1970) Ionic radii for use in geochemistry. Geochimica et Cosmochimica Acta, 34, 945–956.

Zielinski, R. A., Lipman, P. W., and Millard, H. T., Jr. (1977) Minor element abundances in obsidian, perlite and felsite of calc–alkalic rhyolites. American Mineralogist, 62, 426–437.

Manuscript received, January 26, 1982;
accepted for publication, July 26, 1982.